Earthline Journal of Chemical Sciences
E-ISSN: 2581-9003; CODEN: EJCSB4
Volume 9, Number 1, 2023, Pages 47-62
https://doi.org/10.34198/ejcs.9123.4762

Some Tautomers of Dacarbazine - A DFT Study

Lemi Türker

Department of Chemistry, Middle East Technical University, Üniversiteler, Eskişehir Yolu No: 1, 06800 Çankaya/Ankara, Turkey; e-mail: lturker@gmail.com; lturker@metu.edu.tr

Abstract

The present study considers some of dacarbazine tautomers having resulted from 1,3- and 1,5-proton migration. Density functional approach has been adopted at the level of B3LYP/6-311++G(d,p) in order to obtain various geometrical, physicochemical, spectral and quantum chemical properties of the tautomers of concern. Also local aromaticity of the imidazole ring in some of the tautomers having 6π-electrons has been obtained by calculating the nucleolus independent chemical shift values.

1. Introduction

Dacarbazine (dimethyl imidazole carboxamide, imidazole carboxamide, DTIC) is a synthetically produced compound that acts as an alkylating agent following its metabolic activation by liver microsomal enzymes by oxidative N-demethylation to monomethyl derivative that spontaneously decompose to 5-aminoimidazole-4-carboxamid, which is excreted in the urine and diazomethane [1]. The diazomethane then generates a methyl carbonium ion that is believed to be likely cytotoxic species. The major applications of dacarbazine are melanoma, Hodgkin's disease and some soft tissue sarcomas [2,3]. In the later two tumors, its activity is potentiated by doxorubicin, vinblastine or bleomycin [1,4,5]. It causes nausea, vomiting, intestinal symptoms, kidney and liver failure, hair loss, fever and as the delayed toxicity bone marrow depression and anemia, [1,6]. There exist innumerous articles in the literature about the clinical applications of dacarbazine. Also there are various publications on the different aspects of dacarbazine properties [7-12]. When exposed to high temperatures (250-255 °C) dacarbazine decomposes explosively. The 3d metal complexes (cobalt and copper) with dacarbazine were

Received: August 28, 2022; Accepted: September 26, 2022; Published: September 28, 2022

Keywords and phrases: dacarbazine; DTIC; tautomers; chemotherapy; density functional; NICS.

synthesized. Their spectroscopic properties by the use of FT-IR, FT-Raman, and 1HNMR were studied. The structures of dacarbazine and its complexes with copper(II) and cobalt(II) were calculated using DFT methods [13].

Since tautomers having different structures possess dual reactivity, it is anticipated that a material potent to exhibit tautomerism should display variable properties depending on its tautomer content (allelotropic mixture [14]). Note that substances which are isomeric under certain conditions are tautomeric under more drastic conditions [14]. Therefore it would be interesting to put some light on to the tautomerism of dacarbazine.

2. Method of Calculations

All the structures presently considered have been subjected to the geometry optimizations leading to energy minima. The optimizations have been achieved first by using MM2 method which is followed by semi-empirical PM3 self consistent fields molecular orbital (SCF MO) method [15,16] at the restricted level [17,18]. Subsequent optimizations have been performed at Hartree-Fock level employing various basis sets. Afterwards, geometry optimizations were managed within the framework of density functional theory [19,20] at the level of B3LYP/6-311++G(d,p) [17,21]. Note that the exchange term of B3LYP consists of hybrid Hartree-Fock and local spin density (LSD) exchange functions with Becke's gradient correlation to LSD exchange [20,22]. The correlation term of B3LYP consists of the Vosko, Wilk, Nusair (VWN3) local correlation functional [23] and Lee, Yang, Parr (LYP) correlation correction functional [24]. Also, vibrational analyses have been done on the optimized structures. The total electronic energies are corrected for the zero point vibrational energy (ZPE). Moreover, the normal mode analysis for each structure yielded no imaginary frequencies for the $3N–6$ vibrational degrees of freedom, where N stands for the number of atoms in the each system considered. This has indicated that the structure of each molecule corresponds to at least a local minimum on the potential energy surface. All these calculations have been done by using the Spartan 06 package program [25]. Whereas the NICS(0) calculations were performed by using Gaussian 03 program [26].

3. Results and Discussion

Figure 1 shows some of the tautomers of dacarbazine. However, some tautomers, such as tautomerism involved in the amide group itself, is neglected. Some of the tautomeric equilibra shown in Figure 1 result in 1,3 (such as I $\rightleftharpoons$ II) and some in 1,5-type (such as I $\rightleftharpoons$ V) tautomers.

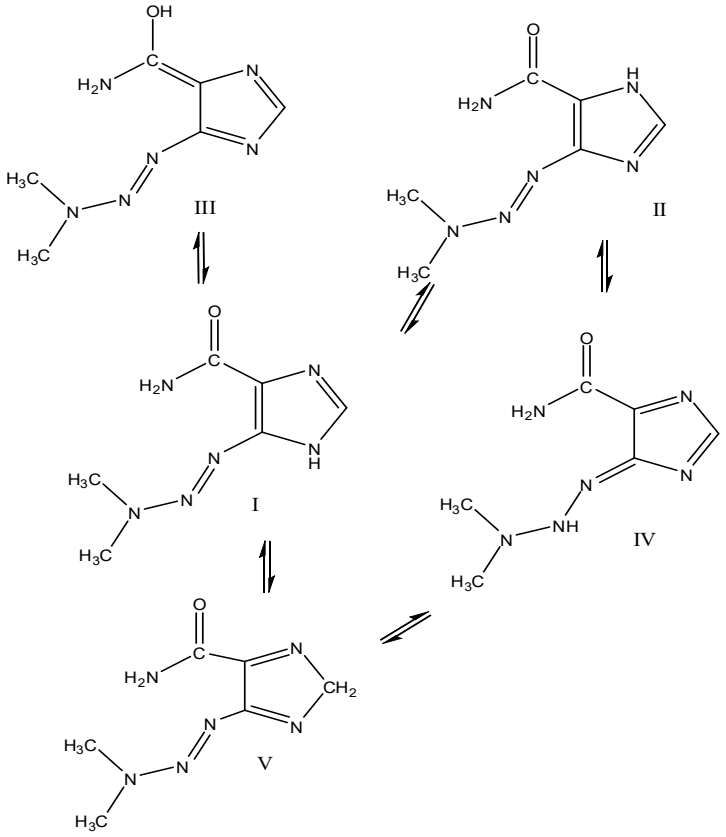

Figure 1. Some of the tautomers of dacarbazine.

Figure 2 shows the optimized structures and the direction of dipole moment vectors of the tautomers considered. It also displays the possible hydrogen bondings (dashed

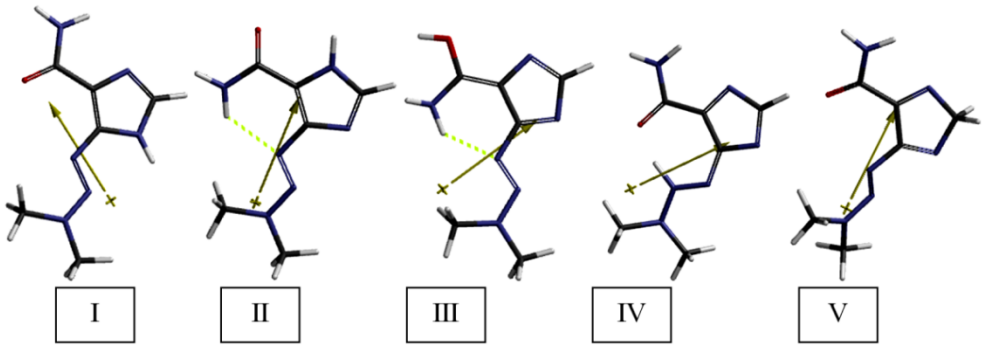

Figure 2. Optimized structures and direction of dipole moment vectors of the tautomers considered.

lines in the figure) predicted by the program. As seen in the figure, direction of the dipole moment vectors exhibits variations from one tautomer to other but generally from somewhere around the dimethylamine moiety to the C=O/COH group. The magnitudes of them are listed in Table 1, together with some other properties. The order of the dipole moments is III>I>IV>II>V. Note that conformation of the substituents, especially the carbonyl moiety is highly different in the optimized structures.

Table 1. Some properties of the tautomers of present interest.

	Area ($Å^2$)	Volume ($Å^3$)	Ovality	Dipole moment	Polarizability	Log P
I	209.92	174.15	1.39	5.58	54.53	-0.93
II	208.31	173.81	1.38	4.43	54.44	-0.93
III	207.45	173.35	1.38	9.05	54.57	-0.34
IV	201.70	171.74	1.35	5.56	54.52	-0.04
V	209.89	174.09	1.39	1.38	54.45	0.97

Dipole moments in debye units. Polarizabilities in 10^{-30} m^3 units

The log P values follow the order of V>IV>III>II=I. Partition coefficients are important property and useful in estimating the distribution of drugs within the body. Hydrophobic drugs with high octanol-water partition coefficients are mainly distributed to hydrophobic areas such as lipid bilayers of cells. Conversely, hydrophilic drugs (having low octanol/water partition coefficients) are found primarily in aqueous regions. Note that in tautomer-V which has the highest log P value has a five-membered ring that is no longer imidazole π-skeleton, and no longer an aromatic system. Tautomer-IV does not have any aromatic ring system but possesses an exocyclic C=N group. In tautomer-III the five-membered ring has lost its aromaticity because of the exocyclic C=N bond.

Figure 3 shows the electrostatic potential (ESP) charges on the atoms of the tautomers considered. It is worth noting that the ESP charges are obtained by the program based on a numerical method that generates charges that reproduce the electrostatic potential field from the entire wavefunction [25].

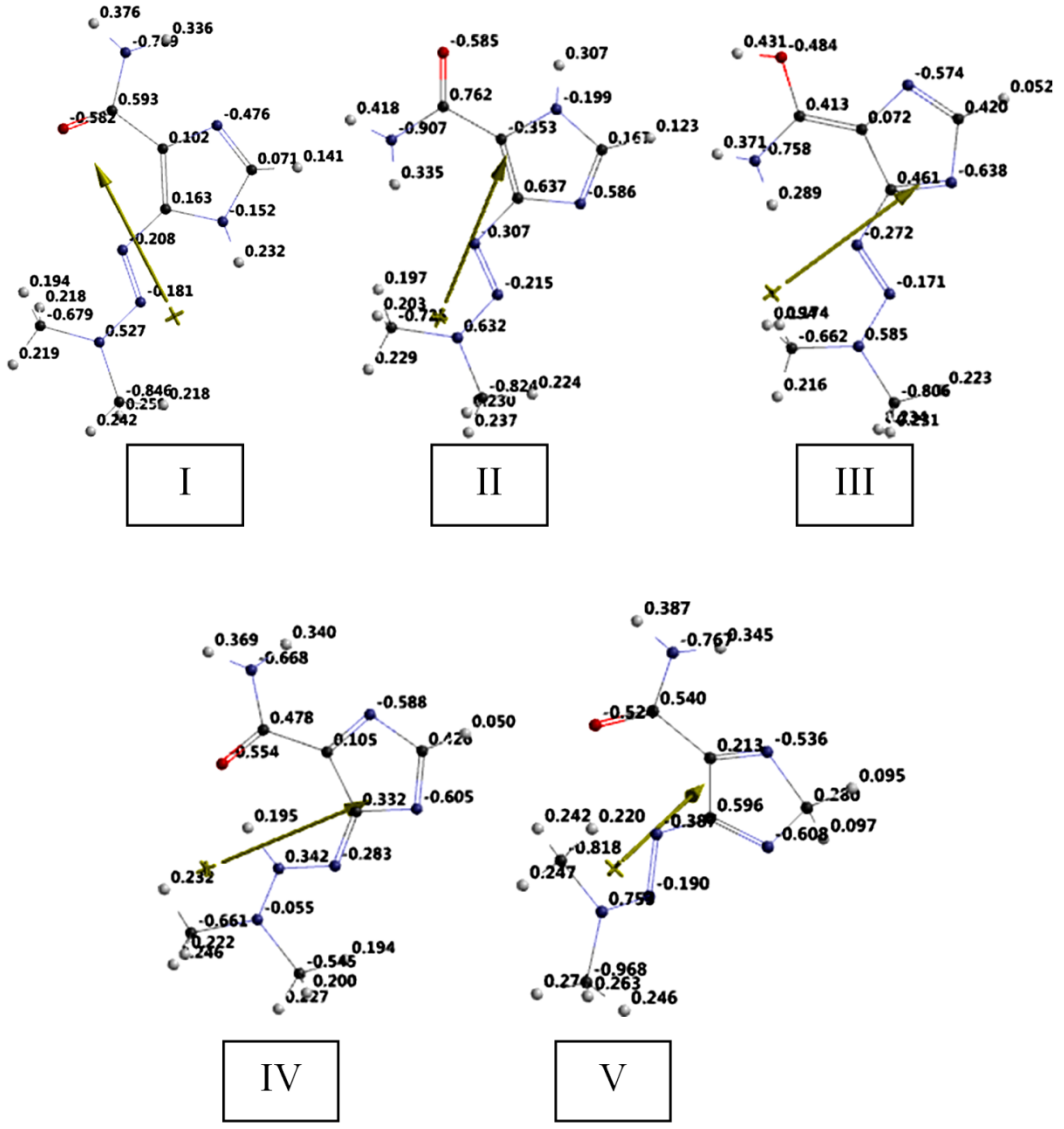

Figure 3. The ESP charges on the atoms of the tautomers considered.

Figure 4 displays the ESP maps of the tautomers considered. As seen in the figure, in most of the cases negative potential region is over/ around the amide oxygen atom or in some cases over one of the imidazole nitrogen atom. The dimethyl amino group resides in positive potential region however intensity depends on the extent of conjugation with the rest of the molecule through the diazo group.

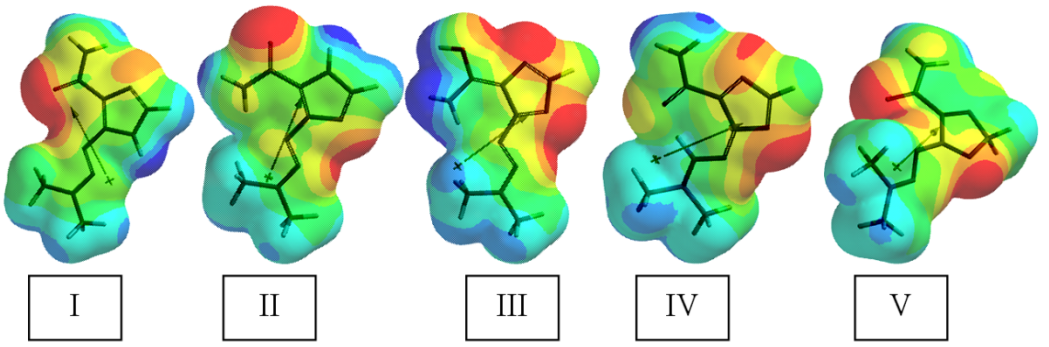

Figure 4. The ESP maps of the tautomers considered.

Calculated IR spectra of the tautomers show distinct N-H stretchings in between 3500-3800 cm^{-1}. The amide N-H vibration for tautomer-I occurs at 3723 and 3581 cm^{-1}. The vibration of tautomeric proton happens at 3646 cm^{-1}. The amide carbonyl C=O stretching appeared at 1739 cm^{-1}. Tautomer-II exhibits a similar spectrum having N-H stretching at 2695 and 3516 cm^{-1} (for amide N-H). The tautomeric proton vibrates at 3624 cm^{-1} and the C=O stretching happens at 1713 cm^{-1}. Tautomer-III has O-H stretching at 3798 cm^{-1} and N-H stretchings at 3605 cm^{-1} and 3372 cm^{-1}. Tautomer-IV possesses amide N-H stretching vibrations at 3709 and 3561 cm^{-1}. The tautomeric proton has N-H stretching occurring at 2354 cm^{-1}. In tautomer-V amide N-H stretchings occur at 3705 cm^{-1} and 3572 cm^{-1} and C=O stretching at 1762 cm^{-1}.

Table 2 lists some energies of the isomers considered where E, ZPE and E_C stand for the total electronic energy, zero point vibrational energy and the corrected total electronic energy, respectively. It also includes the aqueous energies of the tautomers considered. The corrected total electronic energy values follow the order of II<I<IV<V<III. Consequently, tautomers II and III stand for electronically the most and least stable ones, respectively. Tautomer-II is electronically more stable than tautomer-I. The structural differences between them comprise not only the position of hydrogens on the imidazole ring but also conformation of the amide substituent. Also the local aromaticity of the imidazole ring in tautomer-I and II are different (see NICS section below). However, the aqueous energy of tautomer-I is more favorable than that of II. For the other tautomers the stability order in the vacuum and in water exhibits parallelism. In practice, the favorable aqueous stability of tautomer-I over II might be due to favorable intermolecular hydrogen bonding to intramolecular one in the case of tautomer-I.

Table 2. Some energies of the tautomers.

Tautomer	E	ZPE	E_C	Eaq
I	-1676491.71	471.33	-1676020.38	-1676575.30
II	-1676503.41	472.26	-1676031.15	-1676567.43
III	-1676373.73	471.06	-1675902.67	-1676478.44
IV	-1676426.88	470.97	-1675955.91	-1676614.37
V	-1676405.95	469.53	-1675936.42	-1676483.39

Energies in kJ/mol.

Table 3 shows some thermochemical properties of the tautomers considered. As seen in the table, they all have exothermic heat of formation values in the order of II<I<IV<V<III. The entropy values follow the order of I>II>V>III>IV. Note that tautomer-II is a more compact structure as compared to tautomer-I (see Table 1). Consequently, the Gibbs free energy of formation values are in the order of II<I<IV<V<III. The data reveal that tautomer-II is thermochemically more favored in vacuum conditions than tautomer I. The intramolecular hydrogen bonding present in tautomer-II might be one of the reasons for that.

Table 3. Some thermochemical properties of the tautomers considered.

Tautomer	H^o	S^o (J/mol^o)	G^o
I	-1676003.796	434.75	-1676133.418
II	-1676014.773	432.56	-1676143.744
III	-1675886.293	431.93	-1676015.075
IV	-1675940.352	425.19	-1676067.123
V	-1675920.057	432.05	-1676048.873

Energies in kJ/mol.

Figure 5 shows some of the molecular orbital energy levels of the tautomers considered. The tautomers are characterized with distribution of different pattern of inner lying molecular orbital energy levels. Tautomer-IV also differs from the others by having comparatively lower LUMO energy level.

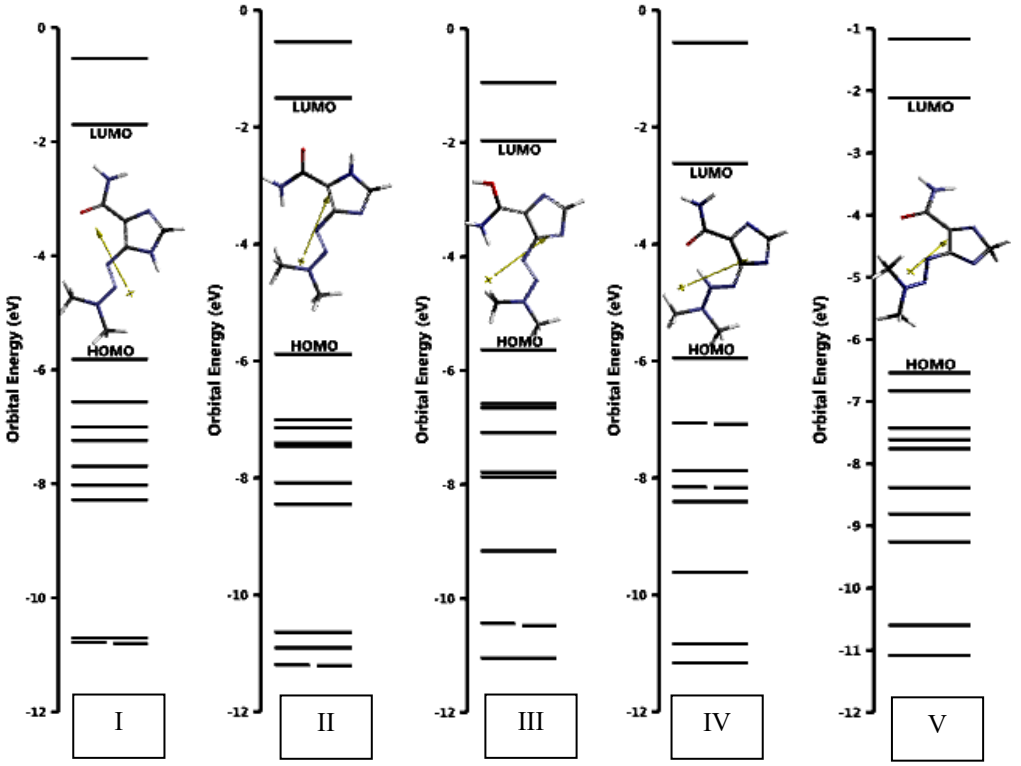

Figure 5. Some of the molecular orbital energy levels of the tautomers considered.

Table 4 shows the HOMO, LUMO energies and the interfrontier molecular orbital energy gap ($\Delta\varepsilon=\varepsilon_{LUMO}-\varepsilon_{HOMO}$) values of the tautomers considered. Orders of the HOMO and LUMO energies are V<IV<II<I<III and IV<V<III<I<II, respectively. As the orders indicate the frontier molecular orbital energies are highly affected by the position of the tautomeric proton. Note that as compared to the others tautomers, tautomer-III (as a better HOMO donor) and tautomer-IV (as a better LUMO donor) are more reactive respectively in reactions involving the tautomers considered and electrophiles and nucleophiles they are reacting.

The interfrontier molecular orbital energy gap values fallow order of IV<III<I<II<V. Tautomer-IV is characterized with the smallest $\Delta\varepsilon$ value in which fulvene-like π-skeleton exists. Note that generally extended conjugation narrows the interfrontier molecular orbital energy gap in conjugated systems [27]. On the other hand, electron donors raise up and electron attractors lower both the HOMO and LUMO energy levels at unequal extents as compared to the parent structure [27]. In the case of tautomerism, as proton

moves from one site to the other, electron density over the system changes so that groups become more or less powerful electron donor or acceptor relative to the previous form. Consequently, the HOMO and LUMO energy levels (thus Δε values) vary from tautomer to tautomer in a rather complex manner.

Table 4. The HOMO, LUMO energies and Δε values of the tautomers considered.

Tautomer	HOMO	LUMO	Δε
I	-561.34	-164.38	396.96
II	-568.02	-144.93	423.09
III	-544.14	-190.13	354.01
IV	-574.42	-253.28	321.14
V	-630.79	-204.41	426.38

Energies in kJ/mol.

Figure 6 displays the HOMO and LUMO patters of the most likely tautomers of the present concern. As seen in the figure both of them have π-symmetry and variation of the position of tautomeric proton does not have any appreciable effect of the patterns of the frontier molecular orbitals.

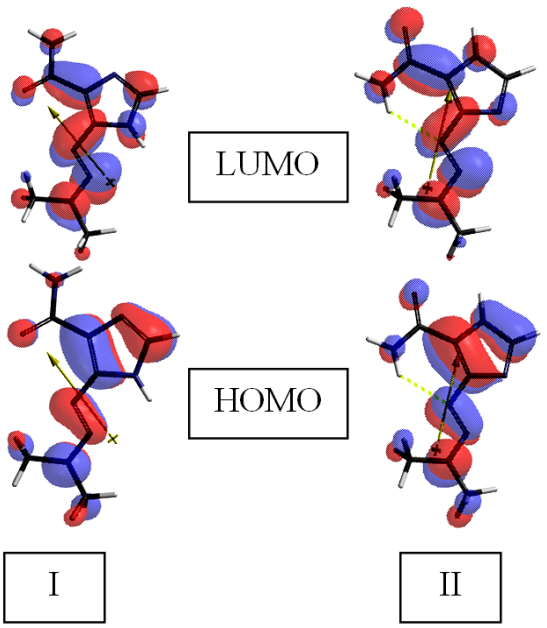

Figure 6. The HOMO and LUMO patterns of tautomers I and II.

Figure 7 shows the time dependent density functional UV-VIS (TDDFT) spectra of the tautomers of present interest. As seen in the figure, they mainly absorb in the ultraviolet region. Tautomers-I and II have very similar spectrums having some slight shift of λ_{max} values. The rest of the tautomers exhibit spectra having either a shoulder or distinct λ_{max} values.

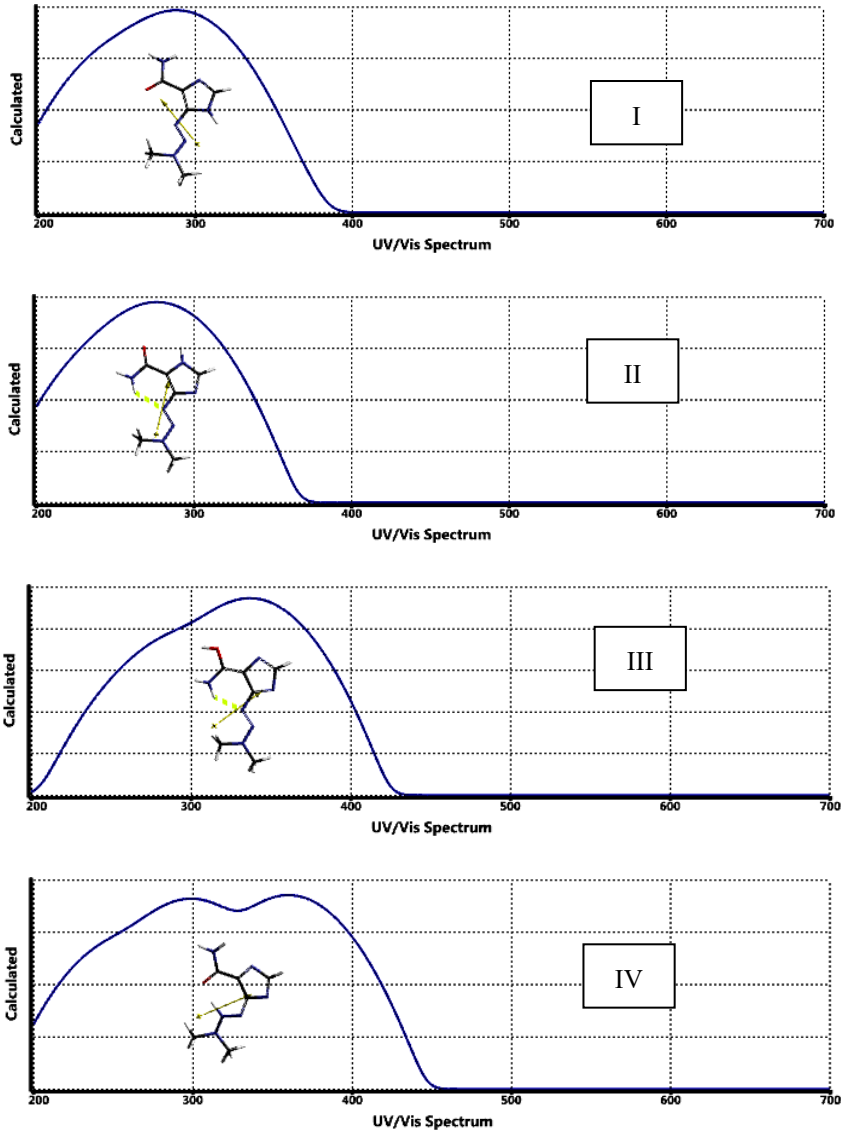

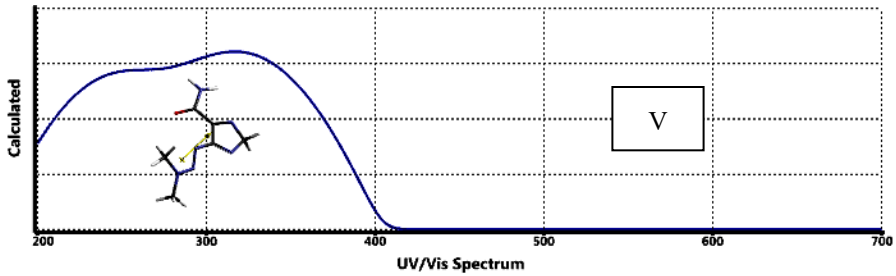

Figure 7. The calculated UV-VIS spectra of the tautomers.

Figure 8 shows the local ionization maps of the tautomers considered. In the local ionization potential map, conventionally red/reddish regions (if any exists) on the density surface indicate areas from which electron removal is relatively easy, meaning that they are subject to electrophilic attack.

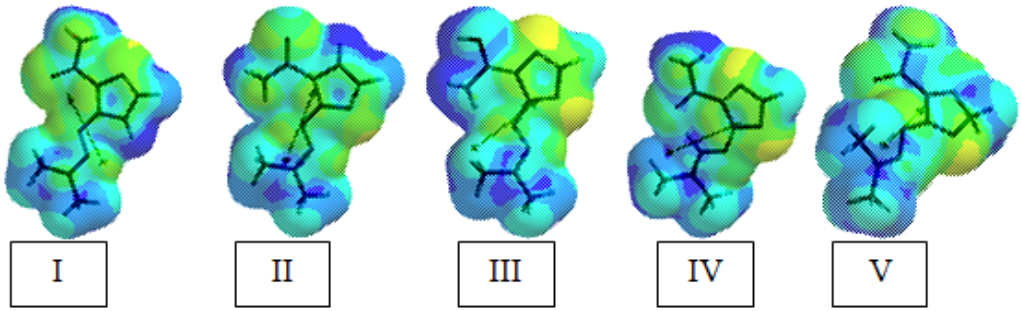

Figure 8. The local ionization maps of the tautomers considered.

Figure 9 shows the LUMO maps of the isomers considered. A LUMO map displays

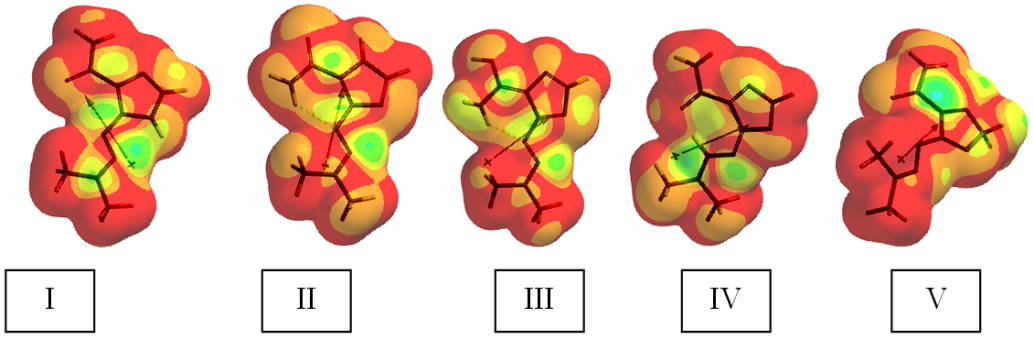

Figure 9. The LUMO maps of the tautomers considered.

the absolute value of the LUMO on the electron density surface. The blue color stands for the maximum value of the LUMO and the color red, the minimum value. so one can guess the sites where nucleophiles attack.

NICS

An efficient probe has been introduced for the local aromaticity which is called "nucleus-independent chemical shift" (NICS) and since then numerous articles appeared exist in the literature, discussing aromaticity in terms of energetic, structural and magnetic criteria [28-39]. NICS is the computed value of the negative magnetic shielding at some selected point in space, generally at center of a ring or cage. The calculated data, so far have piled in the literature through the years have indicated that negative NICS values denote aromaticity (such as -11.5 for benzene, -11.4 for naphthalene). On the contrary, positive NICS values stand for antiaromaticity (28.8 for cyclobutadiene) while small NICS values are indicative of non-aromaticity (-2.1 for cyclohexane, -1.1 for adamantine). However, it is to be mentioned that although NICS approach has been proved to be an effective probe for the local aromaticity of individual rings of polycyclic systems a couple of contradictory results exist [39].

Table 5 shows the NICS(0) values for the aromatic ring in tautomers-I and II. As seen in the table tautomer-I is more aromatic than II. Note that those tautomers have 6π electrons in the ring whereas the other tautomers do not have. Therefore, they are not considered for NICS calculations. Also note that electronically tautomer-II is more stable than I in vacuum but less stable in aqueous conditions. Whereas, thermodynamically G^o values indicate favorability of II over I. The electron topology of tautomer-I should have strengthen the ring current more favorably as compared to II, thus the former one has a more aromatic ring.

Table 5. Nucleus-independent chemical shift (NICS) values of tautomers I and II.

Tautomer	I	II
NICS	-10.8279	-10.5563

4 Conclusion

The present density functional treatment, within the restrictions of the theory and the basis set employed, has indicated that the positional variations of tautomeric hydrogen in dacarbazine backbone result in electronically stable, as well as thermally favorable

systems in all the cases considered. They all have exothermic heat of formation values and the rings having 6π-electrons are highly aromatic. In the present study, positional effect of tautomeric proton on various properties of the tautomeric systems considered have been investigated. They have been found to possess exothermic heat of formation values. They all have favorable Gibbs free energy of formation values and they are all electronically stable. Tautomer-II is more stable than I in vacuum but in aqueous conditions the reverse is true. The NICS calculations indicate that the local aromaticity of tautomer-I is more than II.

References

[1] Katzung, B.G. (1984). *Basic and clinical pharmacology.* Los Altros, California: Lange Medical Pub.

[2] Ahlgren, J.D., & Macdonald, J.S. (1992). *Gastrointestinal oncology*. Philadelphia: J.B. Lippincott.

[3] Rosenberg, S.A., Suit, H.D., & Baker, L.H. (1985). Sarcomas of soft tissue, in V.T. Devita, Jr., S. Hellman and S.A. Rosenberg, eds., *Cancer: Principles and practice of oncology*, 2nd ed., Philadelphia: J.B. Lippincott.

[4] Wu, L-T., Averbuch, S.D., Ball, D.W., Bustros, A.D., Baylin, S.B., & McGuire, W.P. (1994). Treatment of advanced medullary thyroid carcinoma with a combination of cyclophosphamide, vincristine, and dacarbazine. *Cancer*, *73*(2), 432-436. https://doi.org/10.1002/1097-0142(19940115)73:2%3C432::AID-CNCR2820730231%3E3.0.CO;2-K

[5] Edmonson, J.H., Marks, R.S., Buckner J.C., & Mahoney, M.R. (2002). Contrast of response to dacarbazine, mitomycin, doxorubicin, and cisplatin (DMAP) Plus GM-CSF between patients with advanced malignant gastrointestinal stromal tumors and patients with other advanced leiomyosarcomas. *Cancer Investigation*, *20*(5-6), 605-612. https://doi.org/10.1081/CNV-120002485

[6] Glanze, W.D., Anderson, N.K., & Anderson, L.E. (1987). *Medical encyclopedia*. New York: Signet/Mosby,

[7] Radi, A-E., Eissa, A., & Nassef, H.M. (2014). Voltammetric and spectroscopic studies on the binding of the antitumor drug dacarbazine with DNA. *Journal of Electroanalytical Chemistry*, *717-718*, 24-28. https://doi.org/10.1016/j.jelechem.2014.01.007

[8] King, D.T., & Stewart, J.T. (1993). HPLC determination of dacarbazine, doxorubicin, and ondansetron mixture in 5% dextrose injection on underivatized silica with an aqueous-organic mobile phase. *J. Liq. Chromatogr.*, *16*, 2309-2323. https://doi.org/10.1080/10826079308020988

[9] Fiore, D., Jackson, A.J., Didolkar, M.S., & Dandu, V.R. (1985). Simultaneous determination of dacarbazine, its photolytic degradation product, 2-azahypoxanthine, and the metabolite 5-aminoimidazole-4-carboxamide in plasma and urine by high-pressure liquid chromatography. *Antimicrob. Agents Chemother*., *27*, 977-979. https://doi.org/10.1128/AAC.27.6.977

[10] Ordieres, A.J.M., Garcia, A.C., Blanco, P.T., & Smyth, W.F. (1987). An electroanalytical study of the anticancer drug dacarbazine. *Anal. Chim. Acta.*, *202*, 141-149. https://doi.org/10.1016/S0003-2670(00)85909-7

[11] Rodriguez, J.R.B., Costa, A.C., Ordieres, A.J.M., & Blanco, P.T. (1989). Electrochemical oxidation of dacarbazine and its major metabolite (AIC) on carbon electrodes. *Electroanalysis*, *1*, 529-534. https://doi.org/10.1002/elan.1140010609

[12] Shteingolts, S.A., Davydova, V.V., Mar'yasov, M.A., Nasakin, O.E., Fayzullin, R.R., & Lodochnikova, O.A. (2020). Crystal structure of dacarbazine, metoclopramide, and acetylcholine pentacyanopropenides. *J. Struct. Chem.*, *61*, 928-937. https://doi.org/10.1134/S002247662006013X

[13] Swiderski, G., Lazny, R., Sienkiewicz, M., Kalinowska, M., Swisłocka, R., Acar, A.O., Golonko, A., Matejczyk, M., & Lewandowski, W. (2021). Synthesis, spectroscopic, and theoretical study of copper and cobalt complexes with dacarbazine. *Materials*, *14*, 3274. https://doi.org/10.3390/ma14123274

[14] Reutov, O. (1970). *Theoretical principles of organic chemistry*. Moscow: Mir Pub.

[15] Stewart, J.J.P. (1989). Optimization of parameters for semiempirical methods I. Method. *J. Comput. Chem*., *10*, 209-220. https://doi.org/10.1002/jcc.540100208

[16] Stewart, J.J.P. (1989). Optimization of parameters for semiempirical methods II. Application. *J. Comput. Chem*., *10*, 221-264. https://doi.org/10.1002/jcc.540100209

[17] Leach, A.R. (1997). *Molecular modeling*. Essex: Longman.

[18] Fletcher, P. (1990). *Practical methods of optimization*. New York: Wiley.

[19] Kohn, W., & Sham, L. (1965). Self-consistent equations including exchange and correlation effects. *J. Phys. Rev.*, *140*, A1133-A1138. https://doi.org/10.1103/PhysRev.140.A1133

[20] Parr R.G., & Yang, W. (1989). *Density functional theory of atoms and molecules*. London: Oxford University Press.

[21] Cramer, C.J. (2004). *Essentials of computational chemistry*. Chichester, West Sussex: Wiley.

[22] Becke, A.D. (1988). Density-functional exchange-energy approximation with correct asymptotic behavior. *Phys. Rev. A*, *38*, 3098-3100. https://doi.org/10.1103/PhysRevA.38.3098

[23] Vosko, S.H., Wilk, L., & Nusair, M. (1980). Accurate spin-dependent electron liquid correlation energies for local spin density calculations: a critical analysis. *Can. J. Phys.*, *58*, 1200-1211. https://doi.org/10.1139/p80-159

[24] Lee, C., Yang, W., & Parr, R.G. (1988). Development of the Colle-Salvetti correlation energy formula into a functional of the electron density. *Phys. Rev. B*, *37*, 785-789. https://doi.org/10.1103/PhysRevB.37.785

[25] SPARTAN 06 (2006). Wavefunction Inc., Irvine CA, USA.

[26] Gaussian 03, Frisch, M.J., Trucks, G.W., Schlegel, H.B., Scuseria, G.E., Robb, M.A., Cheeseman, J.R., Montgomery, Jr., J.A., Vreven, T., Kudin, K.N., Burant, J.C., Millam, J.M., Iyengar, S.S., Tomasi, J., Barone, V., Mennucci, B., Cossi, M., Scalmani, G., Rega, N., Petersson, G.A., Nakatsuji, H., Hada, M., Ehara, M., Toyota, K., Fukuda, R., Hasegawa, J., Ishida, M., Nakajima, T., Honda, Y., Kitao, O., Nakai, H., Klene, M., Li, X., Knox, J.E., Hratchian, H.P., Cross, J.B., Bakken, V., Adamo, C., Jaramillo, J., Gomperts, R., Stratmann, R.E., Yazyev, O., Austin, A.J., Cammi, R., Pomelli, C., Ochterski, J.W., Ayala, P.Y., Morokuma, K., Voth, G.A., Salvador, P., Dannenberg, J. J., Zakrzewski, V.G., Dapprich, S., Daniels, A.D., Strain, M.C., Farkas, O., Malick, D. K., Rabuck, A.D., Raghavachari, K., Foresman, J.B., Ortiz, J.V., Cui, Q., Baboul, A.G., Clifford, S., Cioslowski, J., Stefanov, B.B., Liu, G., Liashenko, A., Piskorz, P., Komaromi, I., Martin, R.L., Fox, D.J., Keith, T., Al-Laham, M.A., Peng, C.Y., Nanayakkara, A., Challacombe, M., Gill, P.M.W., Johnson, B., Chen, W., Wong, M. W., Gonzalez, C., & Pople, J.A., Gaussian, Inc., Wallingford CT, 2004.

[27] Fleming, I. (1973). *Frontier orbitals and organic reactions*. London: Wiley.

[28] Minkin, V.I., Glukhovtsev, M.N., & Simkin, B.Y. (1994). *Aromaticity and antiaromaticity: Electronic and structural aspects*. New York: Wiley.

[29] Schleyer, P.R., & Jiao, H. (1996). What is aromaticity?. *Pure Appl. Chem*., *68*, 209-218. https://doi.org/10.1351/pac199668020209

[30] Glukhovtsev, M.N. (1997). Aromaticity today: energetic and structural criteria. *J. Chem. Educ*., *74*, 132-136. https://doi.org/10.1021/ed074p132

[31] Krygowski, T.M., Cyranski, M.K., Czarnocki, Z., Hafelinger, G., & Katritzky, A.R. (2000). Aromaticity: a theoretical concept of immense practical importance. *Tetrahedron, 56*, 1783-1796. https://doi.org/10.1016/S0040-4020(99)00979-5

[32] Schleyer, P.R. (2001). Introduction: aromaticity. *Chem. Rev*., *101*, 1115-1118. https://doi.org/10.1021/cr0103221

[33] Cyranski, M.K., Krygowski, T.M., Katritzky, A.R., & Schleyer, P.R. (2002). To what extent can aromaticity be defined uniquely?. *J. Org. Chem*., *67*, 1333-1338. https://doi.org/10.1021/jo016255s

[34] Chen, Z., Wannere, C.S., Corminboeuf, C., Puchta, R., & Schleyer, P. von R. (2005). Nucleus independent chemical shifts (NICS) as an aromaticity criterion. *Chem. Rev*., *105*(10), 3842-3888. https://doi.org/10.1021/cr030088

[35] Gershoni-Poranne, R., & Stanger, A. (2015). Magnetic criteria of aromaticity. *Chem. Soc. Rev*., *44*(18), 6597-6615. https://doi.org/10.1039/C5CS00114E

[36] Dickens, T.K., & Mallion, R.B. (2016). Topological ring-currents in conjugated systems. *MATCH Commun. Math. Comput. Chem*., *76*, 297-356.

[37] Stanger, A. (2010). Obtaining relative induced ring currents quantitatively from NICS. *J. Org. Chem*., *75*(7), 2281-2288. https://doi.org/10.1021/jo1000753

[38] Monajjemi, M., & Mohammadian, N.T. (2015). S-NICS: An aromaticity criterion for nano molecules. *J. Comput. Theor. Nanosci*., *12*(11), 4895-4914. https://doi.org/10.1166/jctn.2015.4458

[39] Schleyer, P.R., Maerker, C., Dransfeld, A., Jiao, H., & Hommes, N.J.R.E. (1996). Nucleus independent chemical shifts: a simple and efficient aromaticity probe. *J. Am. Chem. Soc*., *118*, 6317-6318. https://doi.org/10.1021/ja960582d